the 470-nm emission and the appearance of a structured emission at higher energy which is due to monomer embedded in dimer matrix; this argues against the diffuse 470-nm band being attributed to impurity.

In stretched polyethylene film[22] the absorption of **2** shows a constant dichroic ratio throughout the long wavelength band and is interpretable as due to a single, long-axis polarized, transition. The absorption of **5**, however, shows some structure and the dichroic ratio varies continuously across the band; this may indicate the superposition of two transitions, one of which is long-axis polarized.

In conclusion, the absence of excimer emission from, and the light stability of, crystalline diphenylbutadiene are not intrinsic to the molecule but result from unsuitable packing in the crystal, as in *trans*-stilbene. Our results show that even a molecule which is distorted out of planarity in its ground state may give rise to excimer formation although, unlike previously studied fused-ring compounds, it is quite flexible in fluid media. Although the ground-state geometry of our system has been exactly analyzed by X-ray methods we can only speculate on the question of the geometry of the excimer species. Thus while the molecules are nonplanar in the ground state it is conceivable that they are planar in the excimer. This is a question of considerable interest since it relates to the possibility of using photodimerization in such crystals to generate optically active dimers, a topic which we are investigating in this laboratory.

(22) A. Yogev, L. Margulies, and Y. Mazur, *Chem. Phys. Lett.*, **8**, 157 (1971). We thank L. Margulies of this laboratory for these measurements.

Photodimerization of 9-Anthroic Acid and Sodium 9-Anthroate[1]

Dwaine O. Cowan*[2] and Walter W. Schmiegel[3]

Contribution from the Department of Chemistry, The Johns Hopkins University, Baltimore, Maryland 21218. *Received February 29, 1972*

Abstract: The photodimerization and fluorescence quantum yields of 9-anthroic acid in ethanol and benzonitrile and sodium 9-anthroate in water, deuterium oxide, and benzonitrile were measured at 365 nm as a function of concentration. These efficiencies when coupled with fluorescence lifetime measurements are used to evaluate various mechanistic schemes and to determine the rate constants for the individual steps in the simplest mechanistic scheme that is consistent with our kinetic data.

Changes in substituents and solvents have been observed to produce qualitative and quantitative changes in the rates of reaction and product distributions for numerous thermal but very few photochemical reactions.[4] It has previously been shown that both heavy and light atom solvents can profoundly alter the course of the photodimerization of acenaphthylene.[5] While these solvent effects have been useful in the elucidation of the mechanism of dimerization,[6] it has not been possible to evaluate quantitatively the solvent effect on each of the reaction steps. To learn more about the reaction medium effects on the rates of radiative and nonradiative processes, we have chosen to study the photochemistry of 9-anthroic acid in ethanol and benzonitrile and sodium 9-anthroate in water, deuterium oxide, and benzonitrile.

Anthracene and its many derivatives undergo both relatively efficient dimerization (see Figure 1) and fluorescence.[7] All anthracene dimers formed in solution apparently have the head-to-tail stereochemistry[8] shown in Figure 1. To learn more about the dimerization mechanism for substituted anthracenes and to determine the effect of solvents on the various specific rate constants, we have performed the following measurements: *first*, low-conversion quantum yields of dimer formation as a function of concentration were determined; *second*, relative quantum yields of fluorescence as a function of concentration were measured over the concentration range at which the dimerization was studied; *third*, absolute fluorescence quantum yields in dilute solutions were measured; and *fourth*, the fluorescence lifetimes in dilute solutions were measured.

Results and Discussion

Absorption and Fluorescence Spectra. The absorption and uncorrected fluorescence spectra of 9-anthroic acid (9-COOH) in acidified ethanol and sodium 9-anthroate (9-COONa) in water are shown in Figure 2. The corresponding spectra of the acid and salt in benzonitrile are given in Figure 3.

Whereas a good mirror image relationship of the absorption and fluorescence spectra exists for the sodium 9-anthroate in both water and benzonitrile a very large Stokes shift and an unstructured emission band

(1) Photochemical Reactions. VIII. For part VII, see D. O. Cowan and W. W. Schmiegel, *Angew. Chem.*, **83**, 545 (1971).
(2) Guggenheim Fellow, 1970–1971.
(3) National Science Foundation Graduate Trainee, 1965–1969.
(4) E. M. Kosower, "Physical Organic Chemistry," Wiley, New York, N. Y., 1968; A. A. Lamola and N. J. Turro, "Technique of Organic Chemistry. XIV. Energy Transfer and Organic Photochemistry," P. A. Leermakers and A. Weissberger, Ed., Wiley, New York, N. Y., 1969.
(5) D. O. Cowan and R. L. Drisko, *Tetrahedron Lett.*, 1255 (1967); *J. Amer. Chem. Soc.*, **89**, 3068 (1967).
(6) D. O. Cowan and R. L. Drisko, *ibid.*, **92**, 6281, 6286 (1970).
(7) A. Schönberg, "Preparative Organic Photochemistry," Springer-Verlag, New York, N. Y., 1968.
(8) D. E. Applequist, T. L. Brown, J. P. Kleinman, and S. T. Young, *Chem. Ind. (London)*, 850 (1959); D. E. Applequist, E. C. Friedrich, and M. T. Rogers, *J. Amer. Chem. Soc.*, **81**, 457 (1959); R. Calas, P. Mauret, and R. Lalande, *C. R. Acad. Sci.*, 247, 2146 (1958); O. L. Chapman and K. Lee, *J. Org. Chem.*, 34, 4166 (1969).

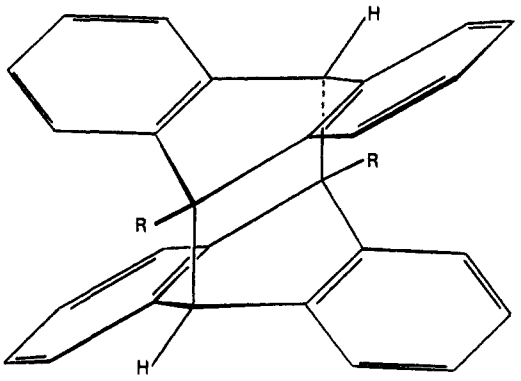

Figure 1. Photodimers of anthracenes.

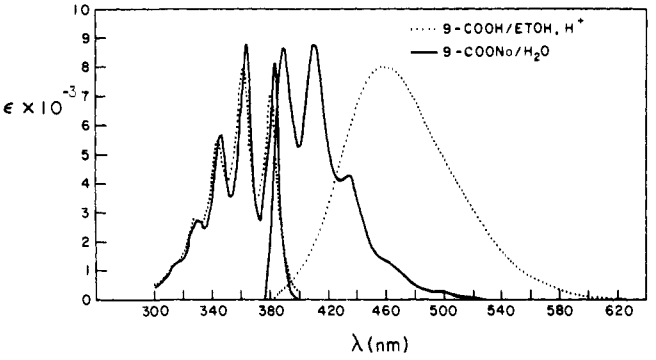

Figure 2. Absorption and fluorescence spectra of 9-anthroic acid in ethanol and sodium 9-anthroate in water.

characterize the acid. The fluorescence emission of the acid was first accounted for on the basis of excimer emission from hydrogen-bonded dimer.[9] Recently some of the esters of 9-anthroic acid[10] have been shown to give absorption and fluorescence emission spectra similar to those observed for the acid. The acid and ester spectra are now[10] interpreted in terms of an excited state rotation of the carboxyl group to a geometry suitable for conjugation with the anthracene ring. Since both the acid and sodium salt have absorption spectra very similar to anthracene, the plane of the carboxyl group must be almost orthogonal to the plane of the anthracene ring in the ground state, and the exciting light used in these dimerization studies (365 nm) must be absorbed by an anthracene-like $^1A \rightarrow {}^1L_a$ transition to produce the $^1B_{2u}$ state. Pariser–Parr–Pople–Mataga (PPPM) calculations[11] on anthracene and the acid indicated that the $^1A \rightarrow {}^1L_a$ transition is primarily a one-electron transition from the highest bonding to the lowest antibonding orbital of the anthracene portion of the molecule. Since sodium 9-anthroate was found to have absorption and fluoresence spectra with good mirror image symmetry the *relaxed* singlet excited state created by 365-nm excitation should have an electron density distribution very similar to anthracene. While the 9-anthroic acid long-wavelength absorption is $^1A \rightarrow {}^1L_a$ in character, the *relaxed*

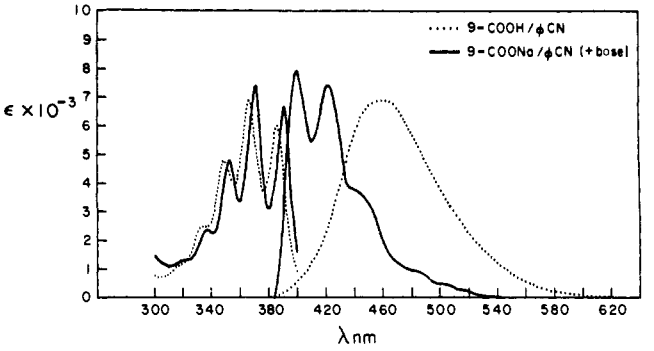

Figure 3. Absorption and fluorescence spectra of 9-anthroic acid and sodium 9-anthroate in benzonitrile.

(rotated carbonyl group) singlet state created by 365-nm excitation must have considerable charge transfer (CT) character.[10,12] To a first approximation a pure CT transition can be considered to be a one-electron excitation from the highest bonding orbital of the aromatic ring to the lowest antibonding orbital of the carboxyl group. Thus, the relaxed excited singlet state of the acid and anion will have different electron density distributions and this difference could alter the rate of dimerization. Fluorescence quantum yields and singlet lifetimes are summarized in Table I. These values are

Table I. Fluorescence Quantum Yields and Singlet Lifetimes

Compound	Solvent	Φ_f ($\times 10^2$)	τ_f, nsec
9-Anthroic acid	Ethanol, H^+	21.8	4.55
	Benzonitrile	64.6	12.3
Sodium 9-anthroate	Benzonitrile	4.88	2.65
	H_2O	6.89	1.50
	D_2O	5.54	1.35
Anthracene	Ethancl		5.55

in reasonable agreement with those in the literature[10] with one exception. The sodium salt in benzonitrile values previously reported are in fact due to the acid in benzonitrile. While this error has been noted[10b] no new values have been reported.

Preparative Photolysis. Solutions of 9-anthroic acid and sodium 9-anthroate in ethanol and water, respectively, were irradiated preparatively using a standard Hanovia 450-W medium-pressure mercury arc lamp and water-cooled immersion vessel fitted with either a uranium glass or Pyrex filter. We could account for 93–97% of the starting acid or salt and observed only 0.3–2.5% of a nonacid material (anthraquinone). Bradshaw and Chapman[13] have reported yields of up to 21% of nonacidic compounds from the preparative photolysis of the sodium 9-anthroate in water. However, under our kinetic reaction conditions not more than 0.7% of nonacidic material was formed while the balance was either the starting acid, salt, or the corresponding dimer.

Dimerization Quantum Yields. The low-conversion quantum yield of dimerization as a function of con-

(9) N. S. Bazilevskaya and A. S. Cherkasov, *Opt. Spectrosc. (USSR)*, **18**, 30 (1965); *J. Appl. Spectrosc.*, 3, 412 (1965); *Zh. Prikl. Spektrosk.*, 3, 548 (1965).

(10) (a) T. C. Werner and D. M. Hercules, *J. Phys. Chem.*, 73, 2005 (1969); (b) *ibid.*, 74, 1030 (1970).

(11) We wish to thank Dr. R. Gleiter and R. Zahradnik for helpful discussions regarding the calculations.

(12) H. Suzuki, "Electronic Absorption Spectra and the Geometry of Organic Molecules," Academic Press, New York, N. Y., 1967; J. N. Murrell, "Theory of Electronic Spectra of Organic Molecules," Wiley, New York, N. Y., 1963.

(13) A. W. Bradshaw and O. L. Chapman, *J. Amer. Chem. Soc.*, **89**, 2372 (1967).

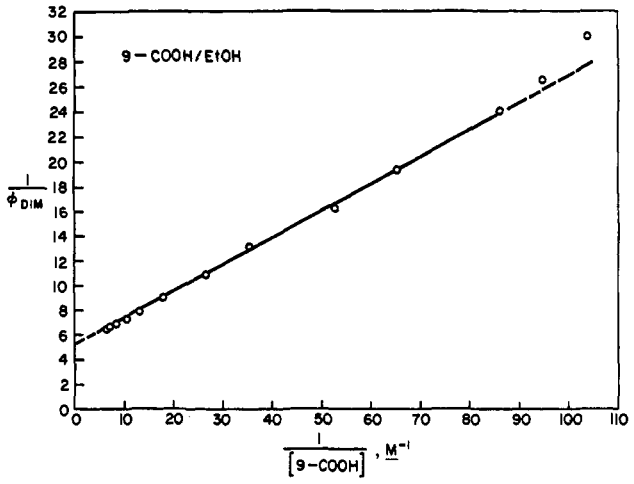

Figure 4. Reciprocal graph of dimerization quantum yield and concentration for 9-anthroic acid in ethanol.

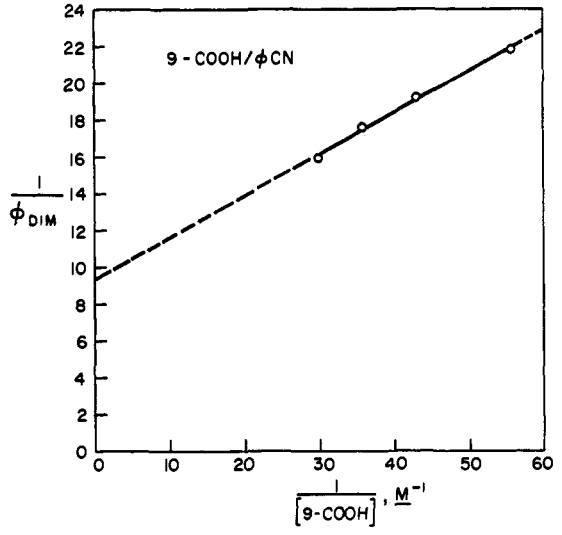

Figure 5. Reciprocal graph of dimerization quantum yield and concentration for 9-anthroic acid in benzonitrile.

centration was determined using 365-nm exciting radiation. The results of these measurements are presented graphically in Figures 4–8 and the relevant slope and intercept values are collected in Table II. Figures 4–8 indicate that plots of $1/\Phi_{DIM}$ *vs.* 1/[C] for the acid and salt give reasonably straight lines. The range of concentrations studied in benzonitrile was limited by the solubility of the acid and salt. The curvature of the sodium 9-anthroate plots at high concentration (0.1 *M*) may be due to some ground-state association. The simple mechanism shown in Chart I is postulated to account for these results.

Fluorescence data ($1/\Phi_F$ *vs.* [A]) to be presented later indicate that triplet dimerization cannot be an important reaction. If reaction 6 (concentration quenching) were neglected then the intercept of a $1/\Phi_{DIM}$ *vs.* 1/[A] plot would be required to be unity (see eq 7). As can be seen from intercepts noted in Table II the relative importance of this reaction varies widely.

(1) Concentration Quenching. Since no observable event results from the required process(es) and its rate is concentration dependent (in the same manner as dimerization), the process is conveniently termed con-

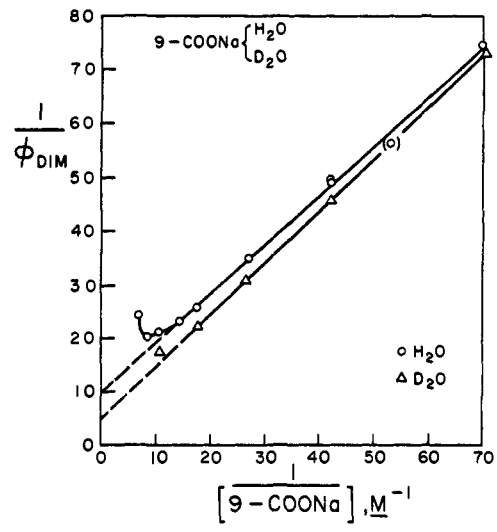

Figure 6. Reciprocal graph of dimerization quantum yield of sodium 9-anthroate in water and deuterium oxide.

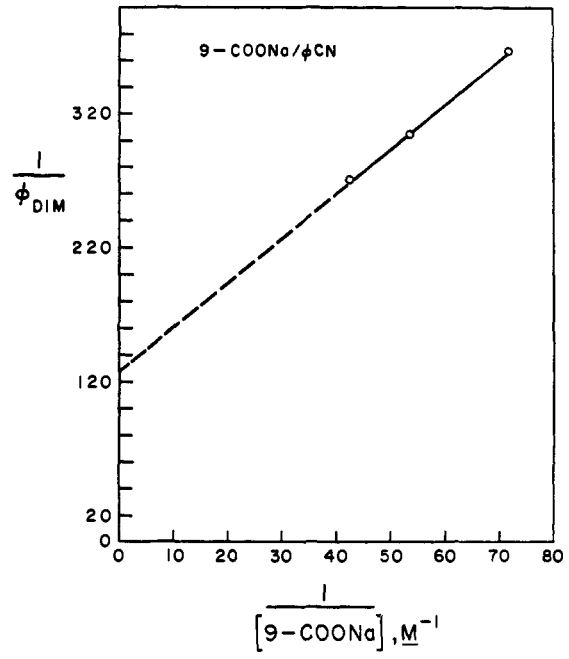

Figure 7. Reciprocal graph of dimerization quantum yield of sodium 9-anthroate in benzonitrile.

Chart I

Process	Rate		
$A + h\nu \longrightarrow A^s$	I_a	light absorption	(1)
$A^s \longrightarrow A + h\nu$	$k_F[A^s]$	fluorescence	(2)
$A^s \longrightarrow A$	$k_{IC}[A^s]$	internal conversion	(3)
$A^s \longrightarrow A^t$	$k_{ISC}[A^s]$	intersystem crossing	(4)
$A^s + A \longrightarrow D$	$k_{DIM}[A^s][A]$	dimerization	(5)
$A^s + A \longrightarrow 2A$	$k_{CQ}[A^s][A]$	concentration quenching	(6)

$$1/\Phi_{DIM} = (k_{DIM} + k_{CQ})/k_{DIM} + [(k_F + k_{ISC} + k_{IC})/k_{DIM}]1/[A] \quad (7)$$

centration quenching. Of the actual process(es) of degradation or transfer of electronic energy at least three major concentration-dependent deactivation mechanisms may be considered: deactivation to the

Table II. Dimerization and Fluorescence Results

Compound	Solvent	Dimerization curve Intercept	Dimerization curve Slope, M	Fluorescence curve F^a	Fluorescence curve Slope,^{b} M^{-1}
9-Anthroic acid	EtOH	5.2	0.215	5.21	117
	PhCN	9.3	0.227	1.82	67
Sodium 9-anthroate	PhCN	128	3.33	30.6[c]	758[c]
				13.5[d]	702[d]
	H_2O	10.0	0.914	6.93[e]	239[e]
				15.6[f]	250[f]
	D_2O	5.0	0.964	7.39[e]	240[e]
				16.7[f]	249[f]

[a] Factor required to convert $1/I_F$ curve into $1/\Phi_F$ curve ($F/I_F^\circ = 1/\phi_F^\circ$). [b] Slope of $1/\Phi_F$ *vs.* [A] curve; slope = $(k_{DIM} + k_{CQ})/k_F$. [c] 420-nm emission. [d] 445-nm emission. [e] 410-nm emission. [f] 435-nm emission.

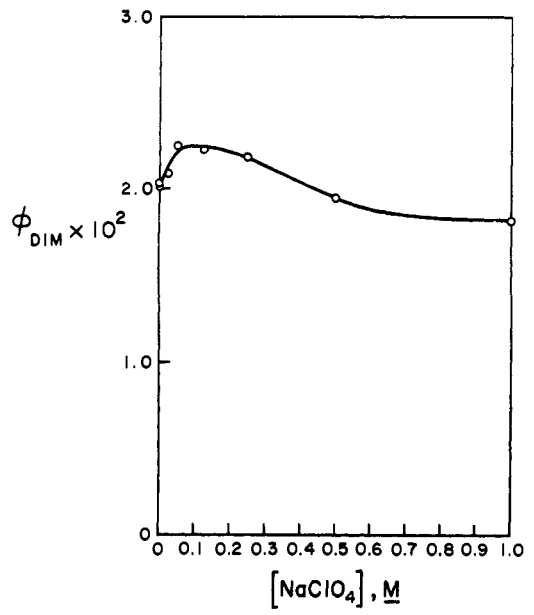

Figure 8. Dependence of dimerization quantum yield of 0.025 M aqueous sodium 9-anthroate on concentration of added sodium perchlorate.

ground state *via* the triplet state through collisions with ground-state solute molecules, formation of excimers followed by their subsequent decay, and formation of unstable covalently bonded dimeric species. While we favor either the excimer or the σ bond diradical mechanism, the following discussion treats each of the three mechanisms as reasonable alternatives.

Concentration-assisted intersystem crossing has been invoked previously in the anthracene area but no compelling arguments for spin reversal due to collisions with non-heavy-atom containing solutes (or solvents) have been advanced.[14] This pathway presently appears unnecessarily speculative, but since it is subject to direct examination *via* flash photolytic triplet counting, the demonstration of its existence or nonexistence will be possible.

The second and third possibilities, excimer formation followed by decay to the ground state and formation of unstable covalently bonded dimeric ground-state species, are probably experimentally indistinguishable in the absence of a new fluorescence band. Since only one emission band was observed for 9-COOH–EtOH as well as for all other systems described in this study, the specific formulation of an excimer-based concentration quenching process is not warranted. Although some examples of excimer fluorescence of anthracene derivatives are known,[15] it seems premature to exclude the possibility of formation of unstable ground-state species. These may be of a diradical character and perhaps reflect the failure to isolate head-to-head mono-*meso*-anthracene dimers if dissociation and decay to ground-state monomers are preferred to cyclization at the 9,9′ positions of any dimeric species bonded at the 10,10′ positions. If a nonfluorescent excimer is formed, its facile nonradiative decay suggests that the potential surfaces of the bound excimer and dissociative unbound ground state intersect or lie sufficiently close at some point to permit tunneling. Furthermore, if the attractive portion of the potential surface were sufficiently deep to impart a lifetime of the order of a few nanoseconds, one might expect excimer fluorescence. The absence of such emission may, therefore, suggest the intermediacy of a rather poorly stabilized excimer or, indeed, a diradical species.

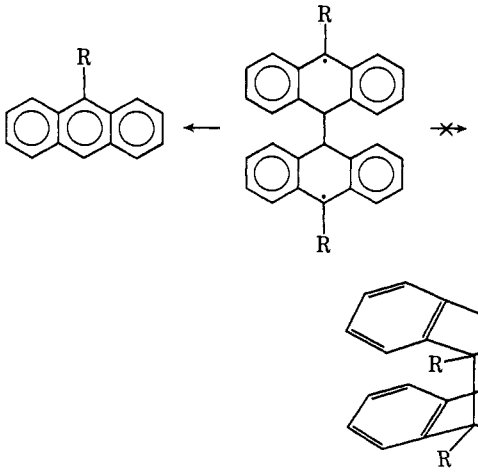

Bowen and Tanner[16] and Cherkasov and Vember[17] proposed concentration quenching of anthracenes involving the triplet state: $^1A + A \rightarrow {}^3A + A$. Livingston[18] formulated concentration quenching as direct deactivation to the ground state: $^1A + A \rightarrow 2A$. Bowen,[19] in a general survey of the photochemistry

(14) E. J. Bowen and J. Sahu, *J. Phys. Chem.*, 63, 4 (1959).

(15) J. B. Birks and J. B. Aladekomo, *Photochem. Photobiol.*, 2, 415 (1963); R. L. Barnes and J. B. Birks, *Proc. Roy. Soc. (London), Ser. A*, 291, 570 (1966); T. Forster, *Angew. Chem.*, 81, 364 (1969).

(16) E. J. Bowen and D. W. Tanner, *Trans. Faraday Soc.*, 51, 475 (1955).

(17) A. S. Cherkasov and T. M. Vember, *Opt. Spectrosc. (USSR)*, 6, 319 (1959).

(18) R. Livingston in "Photochemistry in the Liquid and Solid States," F. Daniels, Ed., Wiley, New York, N. Y., 1960, p 76.

(19) E. J. Bowen, *Advan. Photochem.*, 1, 23 (1963).

Table III. Derived Rate Constants

System	$k_F \times 10^{-7}$ sec^{-1}	$k_{IC} + k_{ISC} \times 10^{-7}$ sec^{-1}	k_{DIM}[a] $\times 10^{-7}$ M^{-1} sec^{-1}	k_{DIM}[b] $\times 10^{-7}$ M^{-1} sec^{-1}	$k_{CQ} \times 10^{-7}$ M^{-1} sec^{-1}	$k_{DIM} + k_{CQ} \times 10^{-7}$ M^{-1} sec^{-1}	$k_{DIFFN} \times 10^{-7}$ M^{-1} sec^{-1}
9-COOH–EtOH, H^+	4.79	17.2	102	108	428	530	613
9-COOH–PhCN	5.24	2.88	35.9	37.9	298	334	532
9-COONa–PhCN	1.84	31.9	11.3	13.5	1440	1451	532
9-COONa–H_2O	4.59	62.1	73.0	112[c]	657	730	739
9-COONa–D_2O	4.17	69.8	76.9	204[c]	307	384	598
Anthracene–PhH[d]	7.4	24.0	100		400	500	1100
9-Me–EtOH[e]	5.56	8.8	220		850	1070	613
9-Et–EtOH[e]	5.85	9.6				708	613
9-*n*-Pr–EtOH[e]	5.68	9.2				670	613

[a] From dimerization, see text. [b] From fluorescence, see text. [c] The $1/I_F$ *vs.* [C] graphs for this system showed some curvature at high concentration not observed for the other systems. When measurements were made at more than one wavelength the table gives an average value for k_{DIM}. [d] From ref 18. [e] From ref 17.

of aromatic hydrocarbons in solution, considered that dimerization and concentration quenching are competitive processes involving an excimer intermediate ^1AA: $^1A + A \rightarrow {}^1AA$; $^1AA \rightarrow A_2$; $^1AA \rightarrow 2A$.

For anthracene itself, the last step of the partial mechanism was considered inoperative since the fluorescence and dimerization quantum yields are complementary.

Thus, the concentration quenching phenomenon has had several interpretations, all of which are subject to uncertainty due to the absence of *direct* measurements of second-order nonradiative decay. The nonfluorescent excimer or unstable product alternatives seem most plausible in the present case, however.

(2) The Role of the Triplet State. The primary processes of many aromatic molecules in solution are dominated by intersystem crossing from the lowest excited singlet state to the triplet manifold. For anthracenes, particularly 9-methyl- and 9-phenylanthracene, measurements of quantum yields of fluorescence and triplet formation in dilute solution have given the result that their sum is unity within experimental uncertainty.[20] Thus, any reasonable mechanism must include the intersystem crossing step: $^1A \rightarrow {}^3A$.

The decay of ^3A in fluid solution is nonradiative and does not significantly involve product formation. Support for the insignificant participation of ^3A in product formation derives from observations of Bäckström and Sandros,[21] who found that the triplet-state biacetyl-sensitized photodimerization of anthracene is quite inefficient. These workers calculated a quantum yield of dimerization of approximately 0.01 under conditions where all the light was absorbed by the sensitizer and where the concentrations of anthracene would have corresponded to a quantum yield of dimerization of about 0.08 in the absence of biacetyl and oxygen. Furthermore, the quantum yield was reported to increase with increasing light intensity, suggesting that triplet–triplet annihilation (and product formation from the resulting singlet state) might be involved.

Livingston[18,22] found that at high intensities such as in flash photolysis the reaction $2\,^3A \rightarrow 2A$ is observable. Presumably the observed second-order disappearance of ^3A is due to triplet–triplet annihilation. In addition, the fluorescence data to be presented in the next section leave little doubt that dimerization proceeds exclusively from reaction between ^1A and A.

(3) Internal Conversion. The evidence available from photooxidation studies on anthracene and 9-methyl- and 9-phenylanthracene[17] indicates that most, if not all, of the first-order nonradiative decay arises from intersystem crossing. However, until direct measurements *via* flash photolysis have been performed we will assume that internal conversion could be an important pathway for deactivation of the 9-anthroic acid and sodium 9-anthroate excited singlet states.

(4) Kinetic Consequences. The mechanism given by eq 1–6 would predict the following relationships (eq 7–10). By combining the fluorescence lifetimes

$$1/\Phi_{DIM} = (k_{DIM} + k_{CQ})/k_{DIM} + [(k_F + k_{ISC} + k_{IC})/k_{DIM}]1/[A] \quad (7)$$

$$1/\Phi_F = (k_F + k_{ISC} + k_{IC})/k_F + [(k_{DIM} + k_{CQ})/k_F][A] \quad (8)$$

$$\Phi_F^{\circ} = k_F/(k_F + k_{ISC} + k_{IC}) \quad (9)$$

$$\tau_F = 1/(k_F + k_{ISC} + k_{IC}) \quad (10)$$

(τ_F), eq 10, and the 10^{-5} M fluorescence quantum yields (Φ_F°), eq 9, the values of which can be found in Table I, it is possible to evaluate the specific rate constants for fluorescence (k_F) and the sums of the nonradiative first-order rate constants for internal conversion and intersystem crossing ($k_{ISC} + k_{IC}$). These values are tabulated in Table III. From the slopes of the $1/\Phi_{DIM}$ *vs.* 1/[A] plots (Table II) and the fluorescence lifetimes, the rate constants for dimerization (k_{DIM}) were evaluated. Rate constants for concentration quenching (k_{CQ}) were obtained from the intercept of the dimerization plots using the previously calculated value of k_{DIM}. The rate constants are compiled in Table III. A composite quantum yield *vs.* concentration curve is presented in Figure 9 for 9-anthroic acid. Such profiles of relative efficiencies of photoprocesses vividly illustrate the competition between singlet state deactivation processes as a function of concentration.

Only two sets of primary data and two sets of derived data exist for each such figure. Whereas Φ_{DIM} and Φ_F were directly determined, Φ_{CQ} was derived from dimerization data. The sum $\Phi_{ISC} + \Phi_{IC}$ was calculated by difference.

Several generalities were observed. For all systems at all concentrations examined, concentration quench-

(20) T. Medinger and F. Wilkinson, *Trans. Faraday Soc.*, 61, 620 (1965).
(21) H. L. J. Bäckström and K. Sandros, *Acta Chem. Scand.*, 12, 823 (1958).
(22) G. Porter and M. Windsor, *Discuss. Faraday Soc.*, 17, 178 (1954).

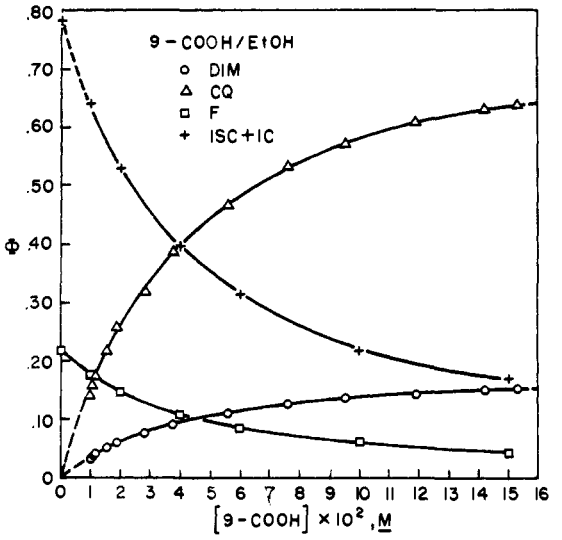

Figure 9. Concentration dependence of composite quantum yields for 9-anthroic acid in ethanol.

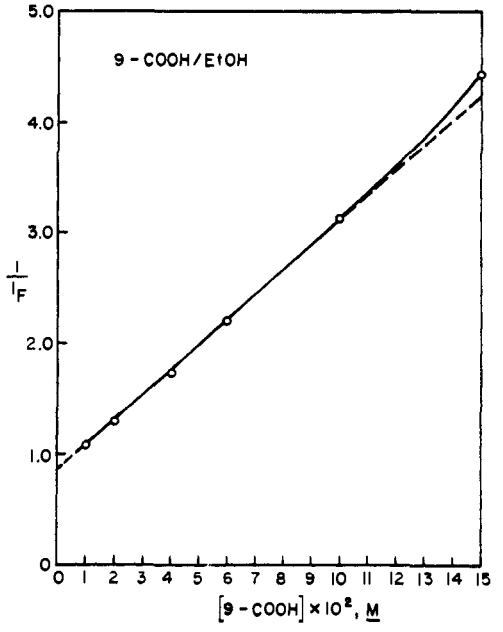

Figure 10. Concentration dependence of reciprocal fluorescence intensity of 9-anthroic acid in ethanol.

ing exceeds dimerization. With the exception of the 9-COOH–PhCN system, intersystem crossing plus internal conversion dominate all paths of deactivation below 2.5×10^{-2} M, and only for this system is fluorescence more probable than intersystem crossing plus internal conversion.

Fluorescence Intensity as a Function of Concentration. The intensity of fluorescence, which is proportional to the fluorescence quantum yield, was measured as a function of sodium 9-anthroate or 9-anthroic acid concentration over the concentration range used in the dimerization studies. These measurements were performed by front surface fluorescence excitation. Typically 99% absorption occurred in less than 0.5 mm of solution when 1×10^{-2} M solutions were excited at the wavelength corresponding to the lowest vibronic transition. The emission was monitored at a wavelength where little, if any, self-absorption occurred.

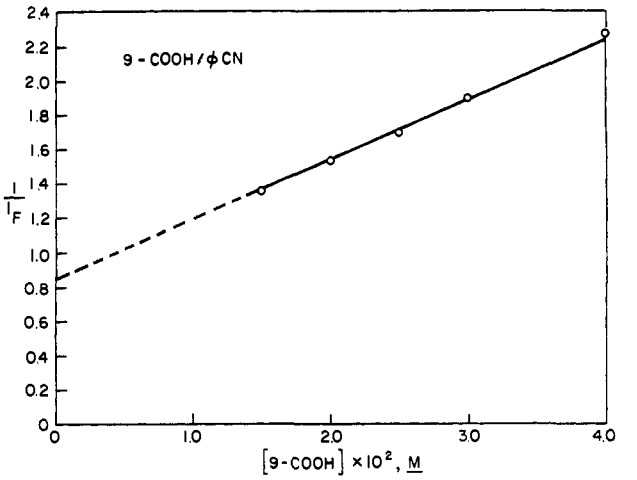

Figure 11. Concentration dependence of reciprocal fluorescence intensity of 9-anthroic acid in benzonitrile.

The graphs of I_F *vs.* 9-anthroic acid concentration are given in Figures 10 and 11.[23] Before the slope can be related to eq 8, the intercept must be given an absolute value ($1/\Phi_F^\circ$) and the experimental slope scaled by the factor (I_F°/Φ_F°). The scale factors and derived slopes are given in Table II. This extrapolation procedure has a large inherent error because the extrapolation is for a line with a large slope over at least two orders of magnitude in concentration. As a result of the errors in this procedure we expect that rate constants derived from the slope will not be as reliable as those from the dimerization data. From the slope of these plots [($k_{DIM} + k_{CQ}$)/k_F] and k_F it is possible to evaluate the sum of $k_{DIM} + k_{CQ}$ independent of the dimerization data. By using the fact that $k_{CQ} = 4.2k_{DIM}$ for the 9-anthroic acid dimerization in ethanol the fluorescence data provide the following values of k_{DIM}: from fluorescence, $k_{DIM} = 108 \times 10^7$ M^{-1} sec^{-1}; from dimerization, $k_{DIM} = 102 \times 10^7$ M^{-1} sec^{-1}. The values of k_{DIM} calculated in this manner are given in Table III.

Because of the good quantitative relationship between fluorescence and dimerization based on the mechanism given by eq 1–6, any mixed dimerization mechanism (singlet and triplet) can be ruled out.

Comparison of Rate Constants. Rate constants determined in this study as well as values from related work are listed in Table III. Since absolute rate constants reflect errors in both fluorescence quantum yields and experimental lifetimes, these values are estimated to be subject to a 25% experimental error. Because specific rate constants represent reaction probabilities per unit time (normalized to unit concentration for second-order rate constants), it is evident that these values, and not quantum yields, are the meaningful indices of absolute reactivity.

The radiative lifetimes ($1/k_F$) of all these systems except 9-COONa–PhCN are in the range 19–24 nsec and consequently their fluorescence rate constants are of very similar magnitude. The exception, 9-COONa–PhCN, is characterized by a considerably longer radiative lifetime (54.3 nsec). The reported[17] radiative lifetimes of three *meso*-alkylanthracenes are very similar (17–18 nsec) and fall at the low end of the lifetime range

(23) Other graphs may be found in the Ph.D. Thesis of W. W. Schmiegel submitted to the Johns Hopkins University, 1970.

defined by the systems other than 9-COONa–PhCN. Literature values of experimentally determined radiative lifetimes of anthracene vary from 20.4 to 21.5 nsec. Thus, k_F values for 9-COOH–EtOH, 9-COOH–PhCN, 9-COONa–H_2O, and 9-COONa–D_2O are quite normal.

Observed values for k_{DIM} vary by an order of magnitude while k_{CQ} values vary only fivefold. The 9-COONa–PhCN system is again conspicuous in that it is characterized by the smallest k_{DIM} and largest k_{CQ} values. The largest k_{DIM} value is that reported for 9-methylanthracene ($220 \times 10^7\ M^{-1}\ sec^{-1}$). Of the present systems only 9-COOH–EtOH appears as reactive toward dimerization as ethanolic anthracene ($k_{DIM} = 100 \times 10^7\ M^{-1}\ sec^{-1}$).

The very low values of Φ_{DIM} of 9-COONa–PhCN are a consequence of the exceedingly large k_{CQ} value and the unusually small value of k_{DIM}. Low values of Φ_{DIM} of 9-COONa–H_2O and 9-COONa–D_2O reflect large values of $k_{ISC} + k_{IC}$ and rather normal values for the remaining rate constants. Values of Φ_{DIM} of 9-COOH–PhCN are reasonably large in view of the low value of k_{DIM} and fairly normal values of k_{CQ} and k_F, because of an exceedingly low value of $k_{ISC} + k_{IC}$.

The observed first-order decay constants can be used to help construct qualitative energy-level diagrams in conjunction with observed 0–0 transition energies. The usual assumption is made that (exothermic) nonradiative transitions occur with a probability which is inversely proportional to the energy separation of the two states involved. For anthracene the existence of a second triplet state of slightly lower energy than the first excited singlet state was theoretically predicted by Pariser[24] in 1956 and experimentally verified by Kellogg[25] in 1966. When these levels are nearly isoenergetic, a thermally activated intersystem crossing rate is observed.[26] This indicates that very small changes in the relative disposition of the energy levels of the first excited singlet and second triplet states is very important. Two energy level diagrams are presented in Figure 12 to qualitatively rationalize reactivities characterized by first-order rate constants describing the deactivation of the singlet states of 9-COOH and 9-COONa. Relative positions of initially reached (Franck-Condon) singlet levels are from absorption spectra, whereas levels corresponding to the fluorescent state (S_F) are from fluorescence spectra. Stokes shifts of about 6 nm are observed for both 9-COONa–H_2O and 9-COONa–D_2O, whereas a 9-nm shift is seen for 9-COONa–PhCN. Neither shift is unusually large. Since no vibrational structure occurs in 9-COOH fluorescence, no 0–0 transition can be assigned. However, if the approximate center of gravity of the fluorescence envelope of structured spectra in the corresponding solvent is approximated by the second vibrational fluorescence maximum (corresponding to the most probable transition in the absorption spectrum), an estimate of the Stokes shift of structureless spectra can be obtained. Thus, for 9-COOH–PhCN the maximum at 460 nm is compared with the "mean" maximum of 9-COONa–PhCN at 420 nm. The 40-nm difference is a crude estimate of the Stokes shift of 9-COOH–PhCN. Similarly, for 9-COOH–EtOH an estimate of 50 nm results from consideration of the "mean" fluorescence maximum of 9-COONa–H_2O at 410 nm and the maximum of 9-COOH–EtOH at 460 nm. Both of these Stokes shifts are unusually large.

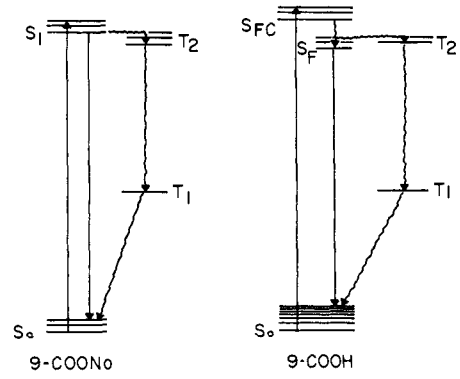

Figure 12. Proposed energy level diagrams for 9-anthroic acid and sodium 9-anthroate.

The unknown levels of the first and second triplet states are positioned relative to the fluorescent level of 9-COONa–H_2O, which has absorption and emission spectra very similar to anthracene and a fluorescence rate constant almost identical with that of the parent species in ethanol. In a sense, then, the 9-COONa–H_2O system is considered to represent "normal" behavior. Since, relative to anthracene, meso substitution is known to lower the energy more for singlet than triplet states[27] and the second triplet energy of anthracene in solution lies slightly below the lowest excited singlet level,[25] the second triplet level of 9-COONa–H_2O is here considered to lie just below the fluorescent level. Due to the large Stokes shift for the 9-COOH systems, the fluorescent state could lie slightly below or at the same level as the second triplet. If we assume that k_{IC} is much smaller than k_{ISC}, then this change in energy levels (and k_{ISC}) would explain the lower values of $k_{ISC} + k_{IC}$ for 9-COOH compared to the 9-COONa systems.

Since dimerization and concentration quenching are second-order processes, it is of interest to consider whether the sum of their rates is diffusion controlled (Table III). All systems except 9-COONa–PhCN are in reasonable agreement with the diffusion constants calculated for the respective solvents at 25° using the modified Debye equation.[28] The high value for 9-COONa–PhCN may reflect an aggregation phenomenon resulting from ion pairing. Thus, if a fraction of ion pairs is associated in groups of two or more and commonly solvated, it is conceivable that effective encounter rates may exceed encounter rates based on the diffusion rate of monomeric solutes. In effect, this would be nothing more than a contribution from static quenching in a measurement which assumes dynamic quenching. The unusually low rate constant for dimerization and abnormally large concentration quenching constant may be reflections of an unfavorable dimerization geometry due to dipolar orientation.

Quite significantly, the dimerization and concentration quenching rate constants for 9-COONa–H_2O and

(24) R. Pariser, *J. Chem. Phys.*, 24, 250 (1956).
(25) R. E. Kellogg, *ibid.*, 44, 411 (1966).
(26) R. G. Bennett and P. J. McCartin, *ibid.*, 44, 1969 (1966); E. C. Lim, J. D. Laposa, and J. M. H. Yu, *J. Mol. Spectrosc.*, 19, 412 (1966); W. R. Ware and B. A. Baldwin, *J. Chem. Phys.*, 43, 1194 (1965).
(27) M. R. Padhye, S. P. McGlynn, and M. Kasha, *ibid.*, 24, 588 (1956).
(28) J. G. Calvert and J. N. Pitts, "Photochemistry," Wiley, New York, N. Y., 1966, p 626.

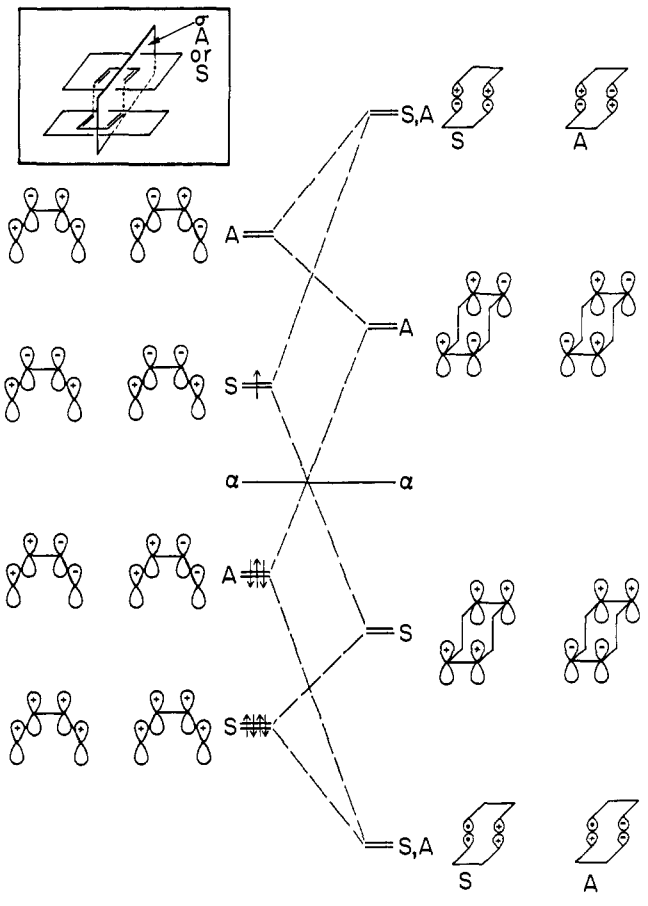

Figure 13. Concerted [$_{\pi}4_s + {}_{\pi}4_s$] dimerization energy level diagram.

9-COONa–D_2O do not reflect the expected coulombic repulsion between anions, whereas rates of some thermal reactions show rather large electrostatic effects, *e.g.*, the rates of formation of three cadmium–bromide complexes vary 50-fold depending on the charge type of the reactants[29] and the rate constants of dimerization of 9-COONa–H_2O and 9-COONa–D_2O fall between those for 9-COOH–EtOH and 9-COOH–PhCN.

The fact that the rate constants for dimerization of 9-COONa–H_2O and 9-COONa–D_2O fall between those for 9-COOH–EtOH and 9-COOH–PhCN also indicates that the change in electron density distribution (see section on Absorption and Fluorescence Spectra) on going from 9-COOH to 9-COO^-Na^+ is either relatively unimportant or compensated for by steric factors.

Figure 8 shows the effect of added $NaClO_4$ on the quantum yield of dimerization of 9-COONa–H_2O at an initial concentration of 0.025 *M*. The yield increases rapidly at low salt concentrations, passes through a maximum at about 0.10 *M*, and slowly decreases at higher concentrations. A quantum yield variation of about 20% is found. Undoubtedly its shape is the result of several effects (reduction of coulombic repulsion, viscosity change).

The nonlinear behavior of plots of reciprocal fluorescence intensity *vs.* concentration of 9-COONa–H_2O and 9-COONa–D_2O indicates that additional modes of quenching of the singlet states of these systems appear at concentrations above 0.06 *M*, where it is probable that multiple equilibria exist between free and associated ions.

Only the concentration quenching rate constant was considerably different in D_2O and H_2O (657 and 307 $\times$ 10^7 M^{-1} sec^{-1}). Even though there is some nonlinearity of $1/\Phi_{DIM}$ *vs.* 1/[C] graphs at high concentrations the k_{CQ}, values which are obtained from the extrapolated curves are still most likely not identical. Bennett and McCartin[26] have also observed no isotope effect upon comparing nonradiative first-order decay constants for 9-methylanthracene and its perdeuterated analog.

Our kinetic data, and their interpretation in terms of the simplest consistent mechanism, do not indicate whether the addition is a concerted ($_{\pi}4_s + {}_{\pi}4_s$) addition as presented in Figure 13 or if a stepwise bond formation is involved.[30] Circumstantial evidence in favor of a concerted reaction has recently been presented by Yang and coworkers.[30a] They observe that the singlet state photoaddition of dienes, *e.g.*, *trans,trans*-2,4-hexadiene, to anthracene occurs in a stereospecific manner.

Experimental Section

Infrared spectra were determined with a Perkin-Elmer Model 337 grating spectrophotometer, ultraviolet and visible spectra were recorded with a Cary Model 14 spectrophotometer, and emission spectra were measured with a Hitachi-Perkin-Elmer MPF-2A fluorescence spectrophotometer. Fluorescence lifetimes were determined with a phase-shift apparatus designed at the Central Research Department of E. I. DuPont de Nemours & Co., Inc., Wilmington, Del.

9-Anthroic acid, obtained from Aldrich Chemical Co., was purified by ether extraction of its aqueous sodium salt, followed by precipitation of the acid with aqueous hydrochloric acid and washing with water. This material was further purified by repeated recrystallization to constant melting point and extinction coefficient. Thus, four recrystallizations from ethanol afforded material melting at 220.0–220.5° dec: uv max (acidified ethanol) 313 (s) nm (ϵ 1170), 328.3 (2750), 344.0 (5430), 360.4 (7970), and 380.5 (7050); ir (KBr) 1685, 1455, 1435, 1290, 1250, 888, 856, 843, 792, 723, and 638 cm^{-1}.

Sodium 9-anthroate, prepared from the purified acid by treatment with aqueous sodium hydroxide and evaporation of water under reduced pressure, melted above 350° and was characterized by: uv max 317 (s) nm (ϵ 1250), 330.0 (2780), 346.0 (5640), 363.7 (8750), and 383.3 (8120); ir (KBr) 1625, 1575, 1445, 1390, 1319, 1277, 889, 865, 771, 731, 657, and 558 cm^{-1}.

Solvents were reagent grade and spectrophotometrically transparent to both filtered excitation and fluorescence wavelengths. Benzonitrile was aniline-free. Deuterium oxide was 99.8% isotopically pure.

Preparative Irradiations. Solutions of 9-COOH and 9-COONa in ethanol and water, respectively, were irradiated preparatively with a Hanovia type L medium-pressure mercury lamp (450 W) fitted with either a uranium glass or "Pyrex" filter to absorb all radiation of wavelengths shorter than 325 and 280 nm, respectively. The water-cooled arc was immersed in the reaction vessel, which was magnetically stirred and continuously flushed with prepurified nitrogen. A side arm of the reaction vessel was capped with a rubber septum, through which nitrogen entered the solution *via* a Teflon hose and nitrogen escaped *via* a short syringe needle. Solutions were also nitrogen-flushed for 15 min before irradiation.

9-Anthroic Acid in Ethanol. A 0.020 *M* solution of 9-anthroic acid in ethanol was prepared from 978 mg (4.40 mmol) of purified acid and 220 ml of solvent. The yellow solution was irradiated through an uranium glass filter for 5 hr as described above. A fine white precipitate formed during the irradiation was kept in suspension by agitation of the stirrer and rising bubbles of nitrogen.

(29) F. S. Dainton and D. B. Peterson, *Proc. Roy. Soc. (London), Ser. A*, 267, 433 (1962).

(30) N. C. Yang and J. Libman, *J. Amer. Chem. Soc.*, 94, 1405 (1972). However, the $4_{\pi} + 2_{\pi}$ photochemical addition of olefins to anthracenes proceeds *via* a stepwise bond formation: J. P. Simons, *Trans. Faraday Soc.*, 56, 391 (1960); G. Kaup, *Chimia*, 25, 230 (1971); N. C. Yang, J. Libman, L. Barrett, Jr., M. H. Hui, and R. L. Loeschen, *J. Amer. Chem. Soc.*, 94, 1406 (1972).

After irradiation the solid material was filtered and dried. The pale yellow filtrate was evaporated and triturated with ether, leaving more of the white solid, which was added to the filter containing the ether-washed original precipitate. The resulting yellow ether solution was extracted with aqueous sodium hydroxide, giving a colorless aqueous phase and a slightly yellow ether phase. Evaporation of ether afforded yellow crystalline material (2.5 mg) which was shown to be virtually pure anthraquinone on comparison of its melting point and infrared spectrum with that of authentic anthraquinone. The basic aqueous phase was acidified with hydrochloric acid, producing a fine yellow precipitate. This was washed with water, dried, and recrystallized from ether by slow evaporation, giving 89 mg of yellow crystals (mp 214–216°) whose infrared spectrum was identical with that of authentic 9-anthroic acid. The combined white solid was washed through the filter with tetrahydrofuran and slowly evaporated to dryness, giving large colorless prisms of photoproduct. This material was dried to constant weight (100°, 30 min), resulting in the formation of 855 mg of white powder (mp 217–219° dec) which could be transformed into highly crystalline 9-anthroic acid by heating a sample contained in a Pyrex ampoule in an oil bath at 180° for 12 hr. The photoproduct had no appreciable ultraviolet absorption above 300 nm and possessed ir (KBr) 1700, 1480, 1460, 1395, 1250, 1205, 1115, 910, 858, 777, 750, 735, 689, and 638 cm^{-1}. Yields were: recovered monomer, 89 mg (9.1%), dimer 855 mg (87.4%), nonacidic material, 2.5 mg (0.3%), material balance, 946.8 mg (96.8%).

Sodium 9-Anthroate in Water. This experiment represents an attempt to repeat an irradiation reported by Bradshaw and Chapman.[13] The only departure from the reported procedure is use of a 450 instead of 550-W Hanovia lamp and use of a separation procedure similar to that described in the previous experiment. A 0.040 *M* solution of sodium 9-anthroate was prepared by dissolving 2.56 g (16.0 mmol) of 9-anthroic acid in 390 ml of an aqueous solution containing 0.64 g (16.0 mmol) of sodium hydroxide and adjusting the pH with drops of dilute hydrochloric acid and sodium hydroxide until pH 9 was attained. This solution was then diluted to 400 ml and irradiated for 5 hr through a Pyrex filter. The initially slightly yellow solution became intensely yellow and also formed a yellow precipitate during irradiation. The color of the irradiated solution persisted overnight in the dark under a nitrogen atmosphere but was discharged within 5 min upon exposure to air while the solution was being vigorously stirred.

The fine yellow precipitate was filtered, giving 0.077 g of a dark yellow solid. The filtrate was extracted with ether after the addition of sodium chloride. Evaporation of ether afforded 0.012 g of a similarly dark yellow solid. The solids were combined and shown to consist principally of anthraquinone upon comparison of the infrared spectrum with that of authentic material.

The extracted aqueous filtrate was warmed to remove residual ether and after cooling was treated with 5% hydrochloric acid to precipitate the acidic solutes. The resulting yellow and white precipitates were washed with water and dried. Trituration of the solid with ether gave a yellow solution and a slightly yellow precipitate. These were separated and the solid was again triturated with ether. This gave a slightly yellow solution and a white precipitate, which was recrystallized from tetrahydrofuran and dried at 100° for 30 min. The resulting white solid (2.77 g, mp 217–219°) possessed an infrared spectrum identical with that of the photodimer of 9-anthroic acid in ethanol. Combination and evaporation of the ether solutions afforded 0.448 g of yellow crystals (mp 218°) whose infrared spectrum was identical with that of 9-anthroic acid. Yields recovered were: recovered monomer, 0.448 g (12.6%), dimer, 2.772 g (77.9%), nonacidic material, 0.089 g (2.5%), material balance, 3.309 g (93.0%).

A similar irradiation based on 3.90 g (16.0 mmol) of solid sodium 9-anthroate in 400 ml of water (0.040 *M*) proceeded indistinguishably and upon identical work-up afforded the following yields: recovered monomer, 0.407 g (11.5%), dimer, 2.944 g (83.5%), nonacidic material, 0.025 g (0.7%), material balance, 3.376 g (95.7%).

Dimerization Quantum Yields. Quantitative irradiations were carried out on an optical bench consisting of a 1-kW high-pressure mercury–xenon short arc lamp (Hanovia 977-B-1) mounted off axis with respect to the axis defined by the aperature–lens–spherical mirror system. The mirror focused the light on a small circular aperture which served as the light source for a 4-in. biconvex quartz collimating lens.[31] The collimated light was filtered through two corning filters (CS-7-37 and CS-0-52) to isolate the Hg 3650-Å lines. The light then passed through the aperture of a cell holder designed to accommodate cylindrical quartz cells of 2 cm diameter and 1 cm length, whose volume was 2.84 ml excluding the filling neck. Stirring was accomplished by placing a small magnetic stirring bar in the filled cell and positioning a magnetic stirrer immediately behind the rear cell face such that the optical and stirring axes coincided. All solutions were preflushed with nitrogen for 15 min and sealed under positive nitrogen pressure before irradiation. This pressure was maintained until the end of the irradiation period.

Relative light intensities were monitored before and after each irradiation by means of a RCA-935 phototube–microammeter combination. The phototube aperature was in the same plane as the front cell face. Frequent standardization of phototube current against absolute light intensities as measured by ferrioxalate actinometry using the previously described cells enabled reliable absolute light intensities to be calculated from phototube measurements. Movement of the phototube across the light beam indicated a high degree of uniformity of intensity within the area of the cell face. The extent of conversion (concentration change) was always kept at 10–15% of the initial anthracene concentration.

The concentration change on irradiation was determined by comparing absorbances at 380.5 nm of two spectrophotometric solutions comprising, respectively, equally diluted, equal volume aliquots of irradiated and unirradiated solution. In this way errors of sampling and dilution are minimized. The ratio of rates of light absorption and of anthracene disappearance at the average concentration is the quantum yield of disappearance at that concentration. The quantum yield of dimerization was computed from the disappearance quantum: $\Phi_{DIM} = 0.5\Phi_{DIS}$. The results are summarized in Figures 4–8 and Table II.

Fluorescence Measurements. Concentrated Solutions ($>10^{-2}$ *M*). A cell identical with that used for photodimerization quantum yields was used for determining fluorescence spectra of nitrogen-flushed and pressurized solutions at photochemical concentrations ($>10^{-2}$ *M*). A solid-sample cell holder enabled a cell to be placed such that its inside front surface is at the intersection of the excitation and emission axes. In this way spectra of very highly absorbing solutions could be measured when the excitation path length was kept very short. Typically 99% absorption occurred in less than the first 0.5 mm of solution when 1×10^{-2} *M* solutions were excited at the wavelength corresponding to the lowest vibronic transition. To preclude significant photolysis the excitation slit width was kept at 2 nm and the signal strength controlled with the photomultiplier sensitivity selector and emission slit width, consistent with requirements for adequate resolution and minimum noise. The direct recording mode was used exclusively.

Fluoresence spectra (excitation wavelength 370 nm) of concentrated solutions ($>10^{-2}$ *M*) were essentially unchanged (except for strong self-absorption of the first vibronic transition in the 9-anthroate ion) from those at "infinite" dilution (10^{-5} *M*). At $>10^{-2}$ *M* there was no evidence of ionization of 9-anthroic acid in ethanol and consequently no need to repress this process by addition of strong acid. Intensity *vs.* concentration data are presented in Figures 10 and 11 and in Table II. The relative intensity measurements were obtained at wavelengths where reabsorption was negligible.

Dilute Solutions (10^{-5} *M*). Fluoresence spectra of dilute solutions were measured in the right-angle mode with care to keep the absorbance of the solutions less than 0.02.

Since the integrated fluorescence spectrum, when plotted as the quanta–second–wave number interval, is proportional to its fluorescence quantum yield, comparison of such spectra of two substances under conditions of equal light absorption permits calculation of the quantum yield of one substance when that of the other is known. Quinine bisulfate in 0.10 *N* sulfuric acid was chosen as the reference system of known[32] absolute quantum yield ($\Phi_F^\circ = 0.50$). The apparent fluorescence spectra obtained from the spectrophotometer were computer corrected for emission monochromator–photomultiplier response, refractive index of the fluorescent solution, change from wavelength to frequency units, and inner filter effects. When more than one excitation wavelength was required to compare the fluorescence quantum yields of a series of compounds whose absorption spectra did not have an acceptable common excitation region, a further correction for the relative spectral distribution of the excitation source–excitation mono-

(31) D. O. Cowan and A. A. Baum, *J. Amer. Chem. Soc.*, **93**, 1153 (1971).

(32) W. R. Dawson and M. W. Windsor, *J. Phys. Chem.*, 72, 3251 (1968).

chromator combination was applied. All of the corrections are required at each wavelength involved in excitation and emission. Flourescence quantum yields are summarized in Table I.

Fluorescence Lifetimes. Nanosecond fluorescence lifetimes of solutions corresponding to those used for determining fluorescence quantum yields were measured on a phase shift instrument using a modulated nitrogen source. Argon instead of prepurified nitrogen was used to flush the fluorometric solutions. The lifetimes measured are reported in Table I.

Acknowledgment. We wish to thank the National Science Foundation for a grant which supported this work. We also thank Professors Roswell and Brand for help with the computer program required to obtain corrected fluorescence spectra and E. I. Du Pont de Nemours & Co. for the use of their phase-shift fluorescence lifetime apparatus.

Mechanism of Acid-Catalyzed Thiolactonization. Kinetic Evidence for Tetrahedral Intermediates

Robert Hershfield[1] and Gaston L. Schmir*

Contribution from the Department of Molecular Biophysics and Biochemistry, Yale University School of Medicine, New Haven, Connecticut 06510.
Received March 27, 1972

Abstract: The thiolactonization of the mercapto acid I in the pH range 0–5 (30°) proceeds *via* acid-catalyzed and pH-independent pathways. The reaction kinetics have been interpreted in terms of a mechanism involving a transition in the rate-determining step at pH 2.94; rate-limiting decomposition of cationic and neutral tetrahedral intermediates at pH >3 gives way to rate-limiting formation of the intermediates at lower pH. Both reaction steps appear to be subject to general acid–base catalysis by carboxylate buffers. The nonlinear dependence of the rate of lactonization of I on formate buffer concentration is suggested to result from self-association of buffer components to form catalytically inactive aggregates. The relevance of the present findings to the concept of "orbital steering" is discussed.

The first evidence for the participation of tetrahedral addition intermediates in thiol ester hydrolysis was obtained with thiol esters derived from trifluoroacetic acid.[2–4] Subsequently, it was shown that the pH–rate profile for the acid-catalyzed hydrolysis of methyl thiolformate could be explained by a mechanism which included tetrahedral intermediates in acid–base equilibrium.[5] The pathways of breakdown of the intermediates generated from ethyl trifluorothiolacetate and methyl thiolformate were found to differ significantly, accounting for the observation that hydrolysis of the former ester was inhibited in acid solution, while that of the latter exhibited acid catalysis.

Although the mechanism advanced for the hydrolysis of methyl thiolformate was in accord with the kinetic data provided, the pH–rate profile of the reaction did not unambiguously rule out other possibilities. It appeared desirable to investigate the hydrolysis of additional aliphatic thiol esters, both to place the favored mechanism on firmer grounds and to obtain quantitative information concerning the effect of structural changes on the modes of breakdown of the tetrahedral intermediates involved in these reactions.

The relatively slow rates of the acid-catalyzed hydrolysis of simple (*i.e.*, not bearing strongly electron-attracting substituents) aliphatic thiol esters at ambient temperature[6] prompted us to undertake the study of acid-catalyzed thiolesterification, whose mechanism should consist of the microscopic reverse of acid-catalyzed thiol ester hydrolysis. To ensure the rapid reaction rates which would allow kinetic study over a wide range of pH, we selected for detailed investigation the thiolesterification of the bicyclic mercapto acid I, whose high reported[7] rate of acid-catalyzed lactonization was well suited to our purposes. To our knowledge, no extended study of thiolesterification has been recorded.

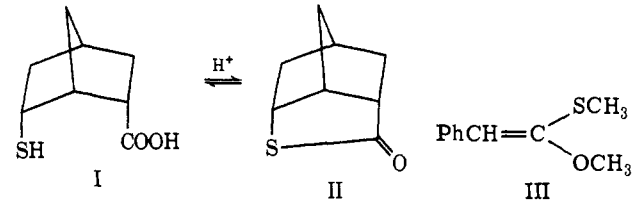

I II III

Results

First-order rate constants for the thiolesterification of the sodium salt of I were determined in aqueous solution, 30°, μ = 1.0 (LiCl), by measuring the rate of increase of absorbance at 243 nm (Table I). At pH >2.7, weak catalysis by formate and acetate buffers was noted, similar to that seen in the hydrolysis of ethyl trifluorothiolacetate.[2] For buffer concentrations rang-

(1) Postdoctoral Research Fellow of the National Institutes of Health, 1971–1972.
(2) L. R. Fedor and T. C. Bruice, *J. Amer. Chem. Soc.*, 87, 4138 (1965).
(3) M. L. Bender and H. d'A. Heck, *ibid.*, **89**, 1211 (1967).
(4) R. Barnett and W. P. Jencks, *J. Org. Chem.*, 34, 2777 (1969).
(5) R. Hershfield and G. L. Schmir, *J. Amer. Chem. Soc.*, **94**, 1263 (1972).
(6) (a) J. R. Schaefgen, *ibid.*, **70**, 1308 (1948); (b) P. N. Rylander and D. S. Tarbell, *ibid.*, 72, 3021 (1950); (c) B. K. Morse and D. S. Tarbell, *ibid.*, **74**, 416 (1952); (d) L. H. Noda, S. A. Kuby, and H. A. Lardy, *ibid.*, **75**, 913 (1953).
(7) D. R. Storm and D. E. Koshland, *Proc. Nat. Acad. Sci. U. S.*, **66**, 445 (1970); D. R. Storm and D. E. Koshland, *J. Amer. Chem. Soc.*, **94**, 5815 (1972).